applied sciences

MDPI

Article

Improvement of the Mechanical Properties by Surface Modification of $ZnCl_2$ and Polydopamine in Aramid Fiber Composites

Guangxian Xu [1], Yinghai Jin [1] and Junhee Song [1,2,*]

[1] Department of Energy Storage/Conversion Engineering, Jeonbuk National University, Jeonju 54896, Korea; xgx1996319@gmail.com (G.X.); syjyinghai@gmail.com (Y.J.)
[2] Division of Convergence Technology Engineering, Jeonbuk National University, Jeonju 54896, Korea
* Correspondence: sjhee@jbnu.ac.kr; Tel.: +82-63-472-2881

Abstract: Although aramid fiber has the advantage of excellent chemical and mechanical properties, the performance of the composites may be reduced due to the low interfacial adhesion between the fabric and the matrix. The surface of the aramid fiber was modified to improve the interfacial properties. The surface of the aramid fibers was treated with $ZnCl_2$ and polydopamine. After the pretreated fabrics were made into a composite material by the vacuum-assisted resin transfer molding (VARTM) process, their mechanical performance was investigated. The highest impact energy was shown in the concentration of 6 wt% $ZnCl_2$ and 1.5 g/L polydopamine, which is 20% better than that of the untreated material. In the bending strength, the condition of 1.5 g/L polydopamine resulted in the highest value and increased by 13% compared to the untreated material. The hybrid surface treatment of $ZnCl_2$ and polydopamine did not significantly affect the tensile strength.

Keywords: aramid fiber; hybrid modification; mechanical properties; Zinc chloride; polydopamine

Citation: Xu, G.; Jin, Y.; Song, J. Improvement of the Mechanical Properties by Surface Modification of $ZnCl_2$ and Polydopamine in Aramid Fiber Composites. *Appl. Sci.* **2022**, *12*, 3119. https://doi.org/10.3390/app12063119

Academic Editors: Dario De Domenico and Farid Taheri

Received: 5 February 2022
Accepted: 16 March 2022
Published: 18 March 2022

1. Introduction

Fabric-reinforced composites have excellent mechanical properties, such as high strength, rigidity, lightweight, corrosion resistance, abrasion resistance and heat resistance [1]. Recently, fabric-reinforced plastic (FRP) composites have been widely used in aerospace, military, automotive industry and sporting goods fields [2]. Carbon, aramid and glass fiber are the keys to determining the excellent performance of the fabric composites, and the structural design has excellent advantages. In recent years, much research work has been devoted to the production of lightweight, high-performance and low-cost polymer composites. However, composites do suffer from some serious limitations. Perhaps the most important of these is the effect of their expensive price and the interfacial bonding between the fiber and resins.

Aramid fibers have excellent flame retardance, light weight, heat resistance, stable chemical properties, radiation resistance and durability. However, since aramid fibers are rigid molecules and have a relatively high orientation and crystallization state, the surface is smooth and inert, so the interfacial adhesion to most industrial composites resins is not good [3]. These shortcomings limit the development of aramid composites. The interfacial adhesion between the fabrics and the resin plays an important role in determining the performance of the structural composites. It was proven that short fibers in the middle plane could change the distribution of delaminations across the thickness so that the delaminations are located near the back of the impact, thus improving residual compression strength and failure strain of CFRPs [4]. Grafted carbon nanotubes improve surface density and enhance adhesion, thus improving the interfacial bonding between the fabric and the epoxy resin collectively while also enhancing toughness [5]. Therefore, it is

the current research trend to enhance the interfacial bond between fiber and resin by means of surface treatment.

Surface decontamination, roughness change and surface activation are the main factors to increase surface free energy and improve adhesion. Additionally, Plasma treatment is beneficial to improve the mechanical properties of fabric-reinforced composites, such as shear strength and impact energy absorption [6–8]. Additionally, different conditions of plasma treatment, such as low-temperature plasma, cold plasma and room temperature plasma, to improve the wettability, roughness, the degree of surface activation are different [9–11]. Sarasini et al. showed the effect of aramid fiber hybridization on the mechanical behavior of basalt fiber-reinforced epoxy resin composites under impact [12]. Behera et al. reported that the tensile strength of the aramid fiber composites put into seawater, 30% concentration of sulfuric acid, and sodium hydroxide, respectively, had different tendencies to decrease with increasing time [13]. Zhong et al. reported that aramid fiber was pretreated with LiCl and then coated with low molecular weight malleated polybutadiene liquid (MLPB) or butadiene-vinyl-pyridine emulsion (VPL) rubber to improve the interfacial adhesion to influence the fatigue behavior of the composites [14].

Ultrasonic treatment can increase interlaminar shear strength (ILSS) of aramid fiber/epoxy resin composites by 13% without reducing the tensile strength [15]. Li et al. investigated the effect of the strength with treatment time and concentration by treating the aramid fiber with $CaCl_2$ ethanol solution. It is proved that Lewis acid treatment can improve the aramid fiber [16]. Lv et al. reported that enhancement of interfacial shear strength by direct fluorination of aramid fiber surface to induce fluorine-related radicals and chemical grafting of carbon nanotubes [17]. Lin et al. reported that Lewis acid treatment etches aramid fibers and increases their surface area and surface activity [18]. Xi et al. and Jia et al. reported that the wettability of aramid fiber surface was enhanced by air dielectric barrier discharge (DBD) plasma at atmospheric pressure [19,20]. Kim and Song enhanced the mechanical strength and stiffness of the fabric composites by immersing the fabrics in an aqueous dopamine solution to increase the interfacial adhesion between the fibric and epoxy resin by depositing PDA on the fibric surface [21].

The Lewis acid treatment effectively enhances the roughness and interfacial adhesion of the fabric surface, while the PDA treatment forms reactive chemical bonds on the fabric surface, which all can enhance the performance of the composite. In this study, in order to improve the interfacial adhesion between the aramid fiber and the epoxy resin, the surface of the aramid fiber was treated with a $ZnCl_2$ solution [22]. The effect of interfacial adhesion was investigated by improving the surface of the aramid fiber by PDA treatment. Chemical reactions were observed by FT-IR to change the content of C=O bonds and N-H bonds on the surface of aramid fibers for surface treatment. Aramid fiber-reinforced polymer (AFRP) was manufactured by the VARTM process, and the mechanical properties of AFRP were studied by tensile, bending and impact tests.

2. Experimental

2.1. Materials

The composites were manufactured using aramid fibers (Kevlar T49, DuPont, Wilmington, DE, USA) of reinforcement and epoxy resins (KFR-120V, KUKDO, Seoul, Korea) as matrix materials as shown in Table 1. Epoxy and the curing agent were mixed at a weight ratio of 5:1. Concentration of 98% Zinc chloride and dopamine hydrochloride and tris (hydroxymethyl)-aminomethane (TRIS) were used in this study. Acetone and 95% ethanol were used to remove dust on the fabric surface and prepare a mixed solution of $ZnCl_2$.

Table 1. Specification of aramid fiber based fabric.

Fiber	Specification
Weave type	Plain woven
Weight (g/m^2)	165
Warp primary fiber	158Tex
Thickness (mm)	0.33 ± 0.025

2.2. Composites Manufacturing

The composites were manufactured by injecting epoxy resin into the Surface-treated fabrics by a vacuum pump using the VARTM process. The average fiber/matrix ratio of the resulting composite is approximately 1:1. Figure 1 shows a schematic of surface modification methods of aramid fiber. First, dust and oil are removed from the fabric surface with acetone, then the first surface modification is performed with one of $ZnCl_2$ or PDA, and finally, the second surface modification is performed with the other one. Table 2 shows the condition of chemical treatment. In the chemical treatment, S, P, Z, 6 and 10 mean silane, PDA, $ZnCl_2$, and the number denotes the concentration (wt%), respectively. The concentration of $ZnCl_2$ was determined by the ratio of the weight of $ZnCl_2$ and ethanol. The concentration of PDA was determined to be 1.5 g/L, which has a good effect on the aramid fibers [21]. All fabrics were cut into a size of 285 mm × 245 mm to make composites.

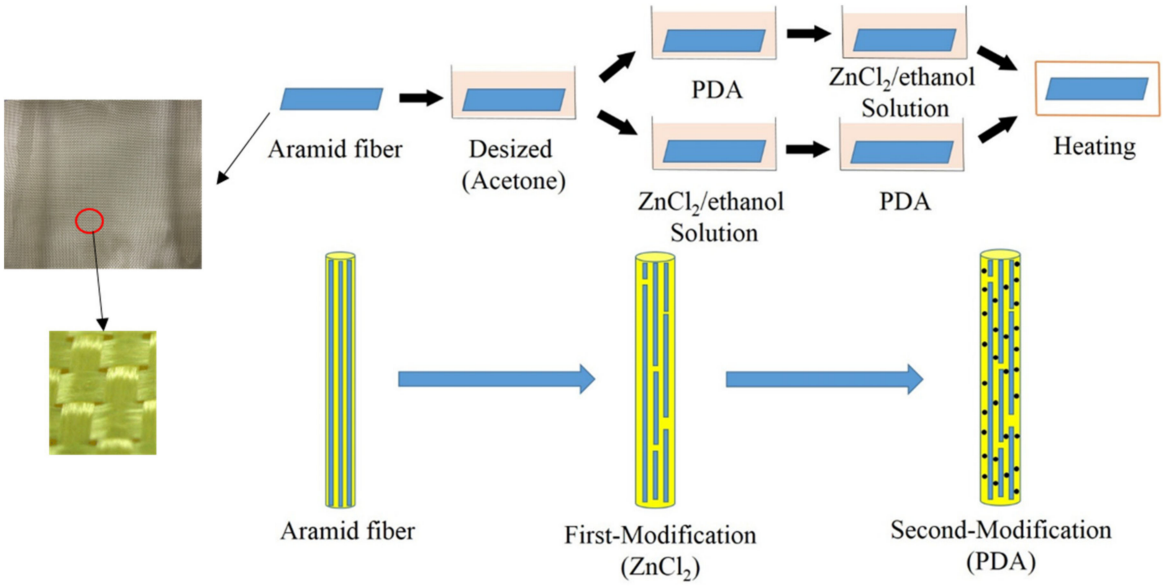

Figure 1. Schematic of the surface modification methods of aramid fiber.

Table 2. Condition of chemical treatment.

Name	Surface Treatment	Agent	Concentration
S	Silane	Silane: Distilled water	10 wt%
P	PDA	PDA, TRIS	1.5 g/L, 40 mM
6Z	$ZnCl_2$	$ZnCl_2$: ethanol	6 wt%
6ZP	$ZnCl_2$-PDA	$ZnCl_2$: ethanol, PDA, TRIS	6 wt%, 1.5 g/L, 40 mM
6PZ	PDA-$ZnCl_2$	$ZnCl_2$: ethanol, PDA, TRIS	6 wt%, 1.5 g/L, 40 mM
10Z	$ZnCl_2$	$ZnCl_2$: ethanol	10 wt%
10ZP	$ZnCl_2$-PDA	$ZnCl_2$: ethanol, PDA, TRIS	10 wt%, 1.5 g/L, 40 mM

Preparation of Solutions

The $ZnCl_2$ solution was prepared based on the weight ratio of $ZnCl_2$ to ethanol. For example, 6 wt% $ZnCl_2$ solution is prepared from 60 g of $ZnCl_2$ and 940 g of ethanol.

The PDA solution is prepared as follows: First, a quantity of distilled water is prepared. Then, TRIS powder was added until pH = 8.5. Finally, dopamine was added and stirred thoroughly with a mixer to allow spontaneous polymerization and uniform distribution of dopamine.

2.3. AF Surface Treatment

Lewis acid treatment generates etching on the fabric surface and increases the roughness of the fabric surface. Dopamine can spontaneously polymerize and deposit a PDA layer on the surface of the aramid fiber. PDA catechol enriched can react with hydrogen bonds. This improves the bonding ability with epoxy resins. Hybrid treatment of these two treatments can further improve the interfacial adhesion between the fabric and the epoxy resin. In order to find the best conditions, surface treatment was performed under various conditions.

In order to remove dust and oil fabrics were immersed in acetone for ten minutes and added to $ZnCl_2$ ethanol mixed solution and modified in 0, 2 wt%, 4 wt%, 6 wt%, 8 wt% and 10 wt% concentrations and 0, 2 h, 4 h, 6 h, 8 h, 10 h and 12 h treatment times. After modification, the aramid fibers were taken out of the solution and washed three times with distilled water. Next, the aramid fiber was added to the prepared PDA solution, shaken for 24 h and dried at room temperature.

2.4. Characterization

2.4.1. Fourier Transform Infrared (FI-IR)

An FT-IR spectrometer (Frontier, Perkin Elmer, Waltham, MA, USA) equipped with an attenuated total reflectance (ATR) UATR reflection accessory was used to determine the chemical bond content of N-H and C=O. The spectra were recorded in the 500–4000 cm^{-1} range with a resolution of 0.4 cm^{-1} to 64 cm^{-1}.

2.4.2. Field Emission Scanning Electron Microscope (FE-SEM)

The morphologies of each aramid fiber and AFRP fracture surface were analyzed by an FE-SEM (Gemini500, Carl Zeiss, Oberkochen, Germany). The images were obtained at a 30 kV acceleration voltage using an upper detector for secondary electrons. All samples were coated with a thin layer of Pt, using an ion sputter coater prior to observations.

2.4.3. Mechanical Properties

Figure 2a–c show the process of tensile, bending and impact experiments. Tensile, bending and impact specimens were cut with water-jet to the sizes recommended in ASTM D638 [23], ASTM D790 [24] and ISO 179 [25]. As shown in Figure 2d, the length of the tensile specimen was 175 mm, the gauge length was 50 mm, the width was 13 mm and the bending specimen was fabricated in size of 80 mm× 12.7 mm. The size of the impact specimen is 80 mm × 10 mm. All specimens were measured 5 times under the same conditions at room temperature. Tensile strength and bending strength were measured by a universal testing machine (Universal testing machine, KD precision, Seoul, Korea). The impact energy of the specimen was measured using an impact testing machine (Pendulum impact testing machine, Wance Technologies Ltd., Shenzhen, China) and the hammer capacity used was 7.5 J. The bending strength was calculated using the following equation:

$$\sigma = \frac{3PL}{2bd^2} \quad (1)$$

where P, L, b and d represent the bending load, support span, width and depth of the specimen, respectively.

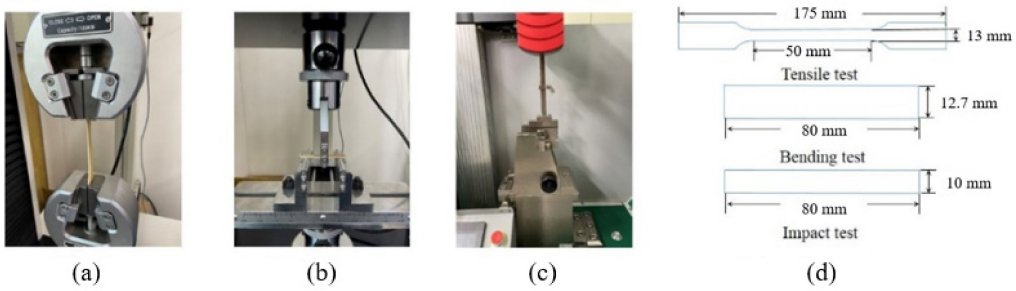

Figure 2. Mechanical properties test and specimens. (**a**) Tensile test, (**b**) Bending test, (**c**) Impact test and (**d**) Specimens picture.

3. Results and Discussion

3.1. Effects of $ZnCl_2$ Treatment on Aramid Fibers

Since there are many aromatic rings that are not easy to move in the molecular structure of the aramid fiber, there are few molecular surface-active groups, so the interfacial bonding strength with the resin matrix is low, which affects the overall performance of the composites. Aramid fibers are treated with $ZnCl_2$ to cause a complexation reaction. The amide group is a potential bifunctional electron donor with 2 lone-pairs electrons on the oxygen and nitrogen atoms, so it has two possible electron donor positions connected to the Zn^{2+} cation. This is advantageous for the coordination of the carbonyl oxygen atom and the metal ion (Zn^{2+}) [26]. As shown in Figure 3, the carbonyl group on the surface of the aramid fiber and the zinc ion are combined to break the hydrogen bond between the N-H and C=O bonds, which are the chemical structures of the aramid fiber. Thus, the NH and CO bond is destroyed by Lewis acid treatment to generate active groups such as N-H and C=O. These active groups may increase the interfacial adhesion between the aramid fiber and the resin yarn. Thereby, the mechanical properties of the composites are improved. The red circle shows the change in the chemical structure of the aramid fiber after $ZnCl_2$ treatment.

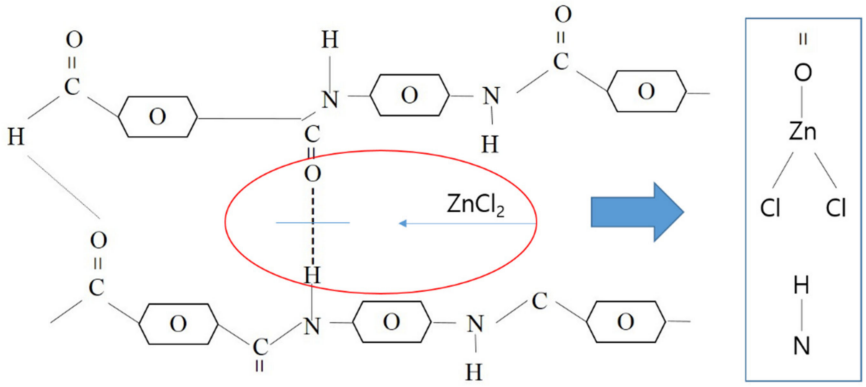

Figure 3. Schematic illustration of hydrogen-bonded sheet structure of Kevlar fiber and $ZnCl_2$-Kevlar complex.

3.2. Surface Structure Analysis by FT-IR

Figure 4 shows the FT-IR analysis graph of the three kinds of Lewis acid surface modifications—$AlCl_3$, $CaCl_2$ and $ZnCl_2$. At wavenumbers 1637 cm^{-1} and 3310 cm^{-1}, we can see the expansion of the vibration peak of C=O (amide I band) and N-H bonds. The chemical composition of the aramid surface was significantly changed after treatment with a Lewis acid ethanol solution. Among three kinds of Lewis acid $AlCl_3$, $CaCl_2$ and $ZnCl_2$, the content of N-H and C=O bonds with $ZnCl_2$ treatment was 3~4% and 5~10% higher than $AlCl_3$ and $CaCl_2$, respectively. The lower transmittance means the higher content of chemical bonds. The N-H and C=O bonds obtained the lowest transmittance under the

$ZnCl_2$ treatment condition. It proves that the $ZnCl_2$ treatment was successful in improving the aramid fiber surface modification because of the high content of N-H and C=O bonds were obtained. Therefore, the $ZnCl_2$ treatment is the best condition in three kinds of Lewis acid surface modifications.

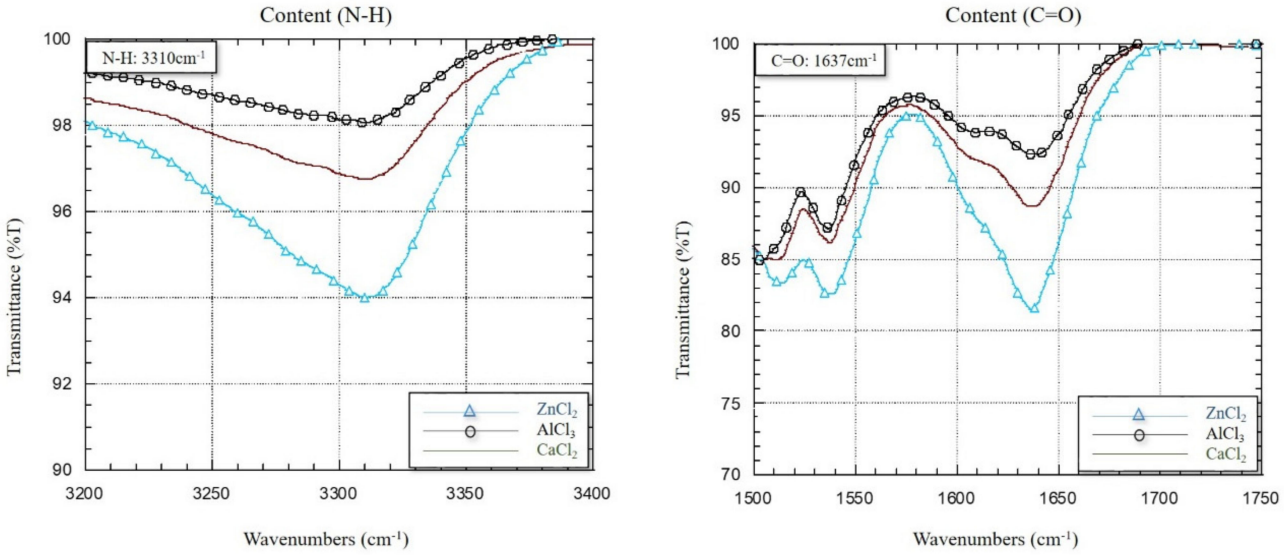

Figure 4. Treatment of aramid fibers with different Lewis acids by FT-IR analysis.

The modification of the $ZnCl_2$ treatment to aramid fibers is determined by the content of active groups, such as N-H and C=O. The concentration and treatment time of the $ZnCl_2$ treatment are important conditions that affect the content of active groups, such as N-H and C=O. Figures 5 and 6 show the results of FT-IR analysis under various concentration (weight ratio) conditions of 2, 4, 6, 8 and 10 wt% and processing conditions of 0, 2 h, 4 h, 6 h, 8 h, 10 h and 12 h. As a result of observing the peak values of the N-H and C=O bonds under the conditions of 2~10 wt% concentration at both wavenumbers 3310 cm^{-1} and 1637 cm^{-1}, the transmittance showed a waveform shape as the concentration increased. Among them, the peak values appeared at 6 wt% and 10 wt%, respectively. Under the treatment of 0~12 h treatment time, the peak value obtained the lowest content of 72.5% by 6 h treatment conditions. The transmittance is 90.82% of the N-H bond and 72.50% of the C=O bond. This is 6% and 18% lower than the 4 h treatment condition, respectively. The content of N-H bonds increased with concentration, but the C=O bonds did show an increasing trend up to 6 wt% and a decreasing trend thereafter. At different treatment times, it also showed an increase in the content of N-H and C=O bonds as the treatment time approached 6 h. This phenomenon may indicate that the contents of N-H and C=O bonds do not increase with time and concentration but rather in a waveform growth manner. So that peak of the maximum increase was found by FT-IR. Additionally, this peak is the position described earlier. Therefore, two concentrations of 6 wt% and 10 wt% and 6 h treatment time were the most beneficial conditions.

3.3. Mechanical Properties

3.3.1. Impact Energy

Figure 7 shows the impact energy of aramid fiber-reinforced polymer (AFRP) composites by $ZnCl_2$ and PDA treatment. The untreated composites showed impact energy of 1.24 J. The highest impact energy of 1.52 J was obtained in the 6ZP condition, which is 20.17% higher than untreated. Compared to the untreated, the impact energy was improved by all single-treated conditions such as S, P, 6Z and 10Z. This is consistent with the evidence that the surface treatment can improve the performance of the composite material by increasing the adhesion between the fabric and the resin. Comparing the impact

energy of the 6PZ, 6ZP and 10ZP hybrid treatment conditions and the 6Z and 10Z single treatment conditions, the hybrid treatment further improved the impact energy by 8%. The $ZnCl_2$ treatment etched the surface of the aramid fiber and improved the roughness. The functionalization of the fabric surface was further improved through PDA treatment. The hybrid treatment improves the interfacial adhesion between the aramid fiber and the epoxy resin. Therefore, the best impact energy was obtained by 10ZP, which implements the PDA treatment after $ZnCl_2$ treatment. The impact energy by PDA-$ZnCl_2$ treatment was lower than $ZnCl_2$-PDA treatment. Because in the PDA-$ZnCl_2$ treatment condition, dopamine adhered to the fabric surface is washed away, which may reduce performance.

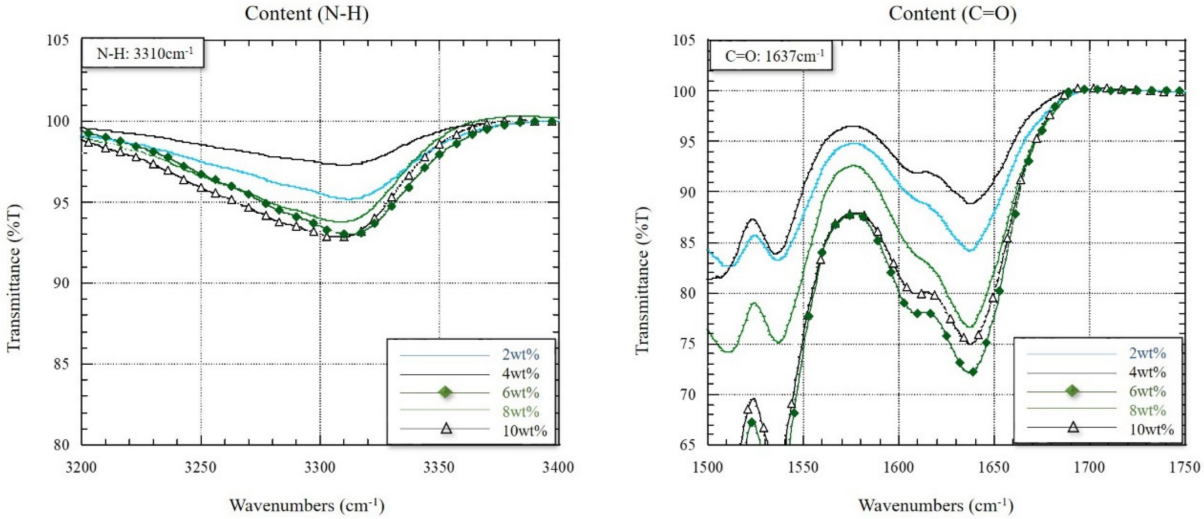

Figure 5. FT-IR analysis of $ZnCl_2$ surface-treated aramid fabrics in various concentrations.

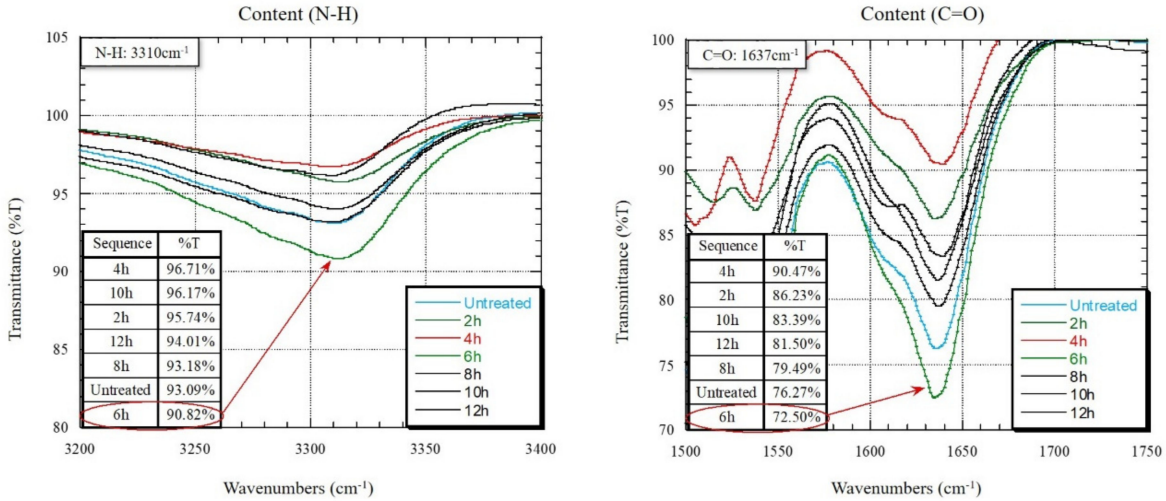

Figure 6. FT-IR analysis of $ZnCl_2$ surface-treated aramid fabrics in various processing times.

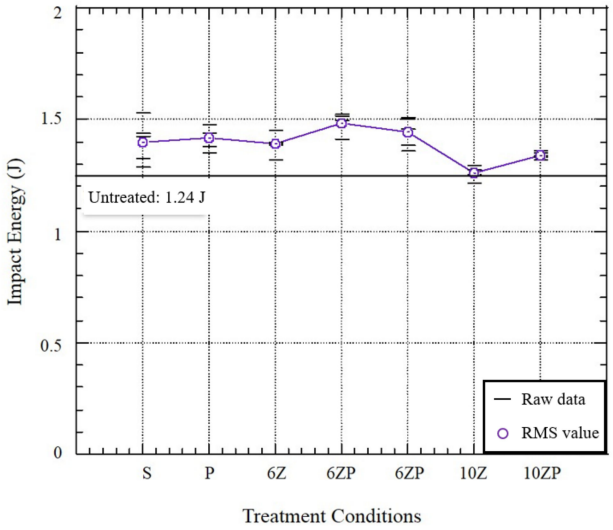

Figure 7. Impact energy of 6-layer aramid fabric under various conditions.

3.3.2. Bending Strength

Figure 8 shows the bending strength of AFRP composites by $ZnCl_2$ and PDA treatment. In untreated conditions, the bending strength of the AFRP was 219.09 MPa and the best bending strength was obtained by P condition (247.85 MPa, increased by 13.13%). As a result of the single-treated conditions that were treated by S, P, 6Z and 10Z, the bending strength improvement trend for aramid fiber composites was P ≥ S ≥ Z. $ZnCl_2$ treatment obtained the lowest improvement in bending strength among the three treatments. Because $ZnCl_2$ treatment can improve bonding ability with resin by giving an etching effect to the aramid fiber surface, the performance improvement rate is reduced by lowering the performance of the fabric itself. Hybrid treatment conditions showed overall performance degradation. Among them, condition 6ZP obtained lower bending strength than condition 6PZ. Under the same hybrid treatment sequence condition, the 10ZP condition with a high $ZnCl_2$ concentration can obtain higher bending strength than the 6ZP condition. Therefore, in the hybrid condition, the bending strength is in the order of 6PZ ≥ 10ZP ≥ 6ZP.

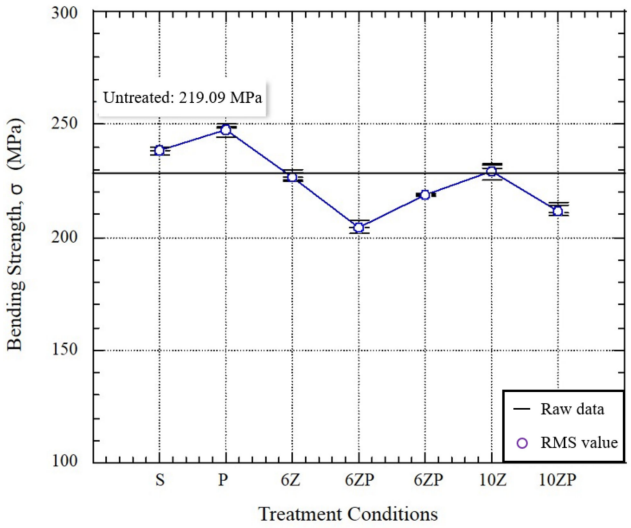

Figure 8. Bending strength of 6-layer aramid fabric under various conditions.

3.3.3. Tensile Strength

Figure 9 shows the tensile strength of AFRP composites by $ZnCl_2$ and PDA treatment. The tensile strength of the untreated condition was 409.39 MPa, and the highest tensile strength was obtained in the 6Z condition (423.74 MPa). This is a 3.51% improvement over the untreated 409.39 MPa. Similar tensile strength improvements were obtained under all treatment conditions. The highest tensile strength was obtained under 6Z conditions, and the lowest tensile strength was obtained under 10ZP conditions. Additionally, the difference between these two conditions is less than 5%. Tensile strength is related to the performance of the fabric itself. Lewis acid treatment weakens the fabric itself by etching the fabric surface, reducing the performance of the composites. However, etching can increase the surface roughness of the fabric and improve the interfacial adhesion between the fabric and the epoxy resin, thereby improving the performance of the composites. It is judged that there is no change in tensile strength as the two phenomena are canceled out.

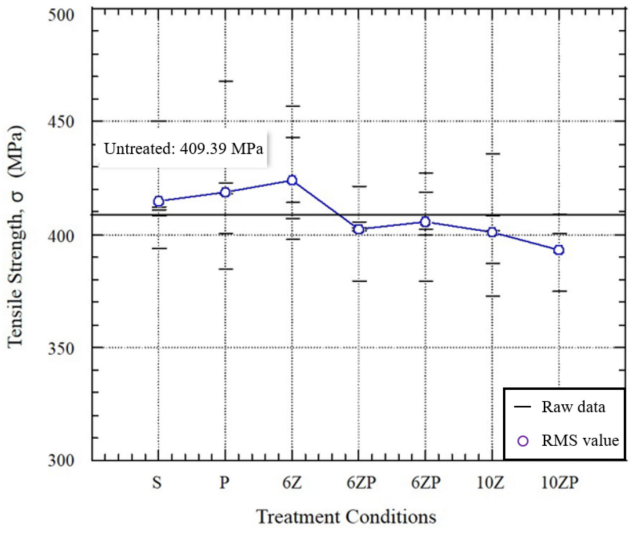

(**a**)

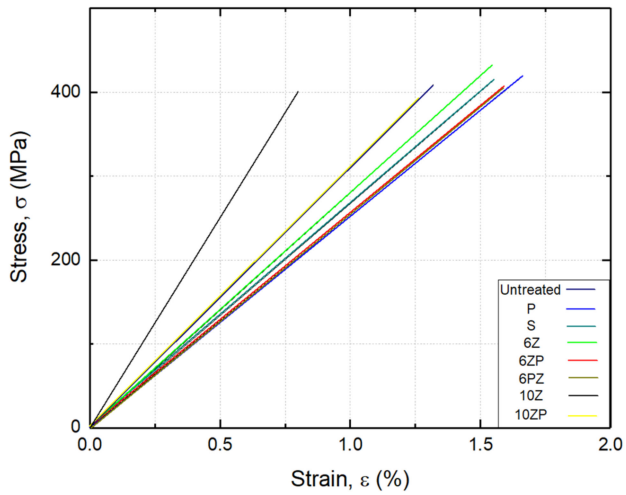

(**b**)

Figure 9. Tensile strength and stress–strain curve of the 6-layer aramid fabric under various conditions. (**a**) Tensile strength, (**b**) Stress-strain.

From Figures 8 and 9a, it can be seen that the tensile and bending strength exhibit different trends, respectively. The overall trend of tensile strength is not very obvious

because the properties of the fabric itself are the key to the tensile strength. Therefore, the variation of tensile strength is within 5% for all conditions. However, in bending strength, it can be seen that the properties of the Lewis-acid-treated conditions are all inferior to the PDA-treated conditions. As explained before, although etching helps to improve the bonding ability with the resin, it reduces the properties of the fabric itself. Thus, the Lewis-acid-treated condition did not perform as well as the PDA-only condition.

It can be seen from the stress–strain curves of the 6-layer aramid fabric under various conditions in Figure 9b that there is a decrease in elongation at 6Z and 10Z for the two conditions treated with $ZnCl_2$ compared to the untreated condition. This may be due to the disruption of the polyamide mechanism in the fabric structure by the $ZnCl_2$ treatment. It can also be seen that all PDA-treated conditions effectively improved elongation. Because the PDA treatment promotes the activation of the fabric surface to enhance the interfacial bonding between the fabric and the epoxy resin. It can be concluded that $ZnCl_2$ and PDA treatment can reasonably compensate for each other's effects on elongation, thus ensuring the mechanical properties of AFRP.

3.3.4. FE-SEM Observation

Figure 10 is SEM images of surface treatment with $ZnCl_2$ for 0–12 h treatment times. We obtain different surface images with $ZnCl_2$ treatment times. (a) is the untreated aramid fiber surface image. It was clean and smooth. (b), (c) and (d) are surface images of aramid fibers treated with $ZnCl_2$ for 2 h, 6 h and 10 h, respectively. A similar image was obtained by (a) and (b). Because the 2 h treatment was too short, the fabric surface was not treated enough. Conditions (c) and (d) showed a remarkable etching effect on the fabric as the surface was changed. However, in condition (d), which is treated for 10 h, the fabric surface was separated by the destruction of the fabric itself as well as etching. This destruction phenomenon can affect the mechanical performance of the fabric composites. It can be seen that the effect received by the fabric surface grows with the treatment time. Because the Lewis acid treatment causes an etching effect on the fabrics, the long treatment time will have some effect on the fabrics themselves. In the surface treatment, the (c) condition, in which etching was appropriate and the fabric itself was not destroyed, was selected as an excellent condition.

Figure 11 shows a $ZnCl_2$-treated SEM image on the surface of the fiber. Comparing the conditions of (a) and (b), the material treated on the fiber surface under condition (b) was remarkably observed. This proves that PDA was coated on the fiber surface under condition (b). The difference between (b) and (c) is the difference in the treatment order of polydopamine and $ZnCl_2$. The amount of PDA adhering to the surface in condition (c)was smaller than condition (b). Because dopamine could be drained in the process of $ZnCl_2$ treatment if the processing order is $ZnCl_2$ first and then PDA. In (b) and (d), the fiber surface etching phenomenon of the high concentration (d) condition is more pronounced than the low concentration (b) condition. It can be seen that the concentration affects the degree of fiber surface treatment. However, the fiber surface under condition (d) has a high etching effect, and the fiber itself may be damaged, resulting in a decrease in performance.

Figure 12 shows the fracture surface of each composite after the Impact test. As in image (a), the impact fracture surface of the untreated aramid composites was often cracked between the fiber and the resin. However, under the conditions of (b), (c), (d) and (e), the cracking phenomenon is significantly reduced. Among them, there was still some cracking in condition (b) with only $ZnCl_2$. (c) and (d) conditions, in which the hybrid treatment was performed, were not only cracked but also had fewer gaps between the fibers and the resin. Condition (e), which was treated at a concentration of 10 wt%, was no cracking after receiving an impact force between the fiber and the resin, but it was found that the fiber itself was destroyed. It is judged that the performance of the composites decreases due to the separation and destruction of the fiber itself because of a high concentration.

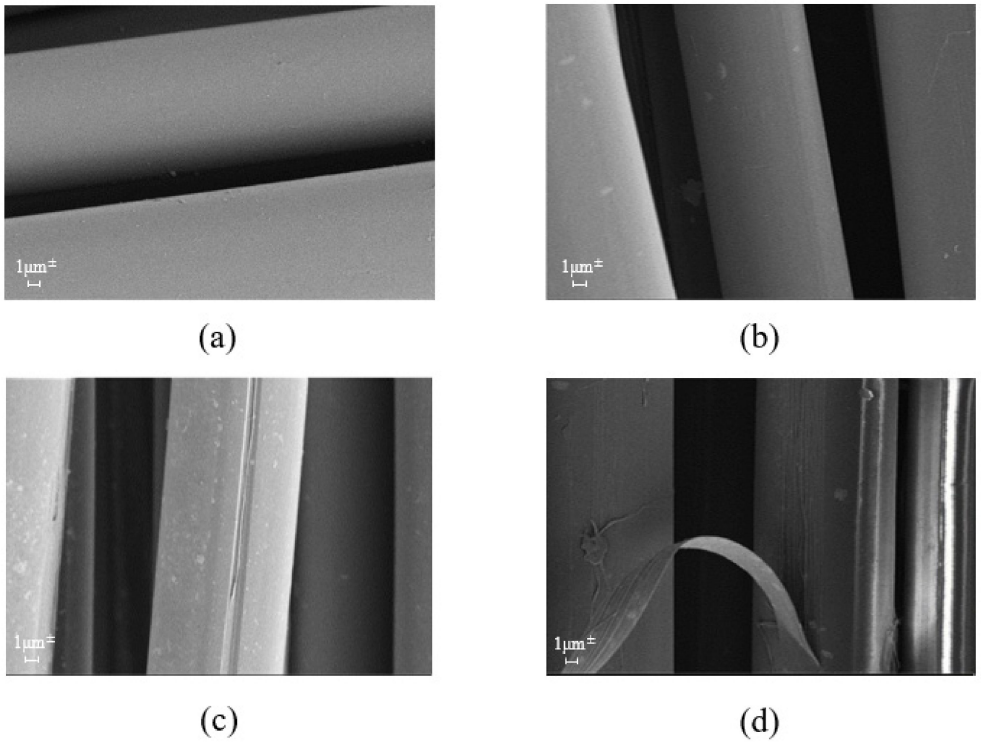

Figure 10. SEM images of the surface treatment with the $ZnCl_2$ treatment time. (**a**) Untreated, (**b**) 2 h, (**c**) 6 h (**d**) 10 h.

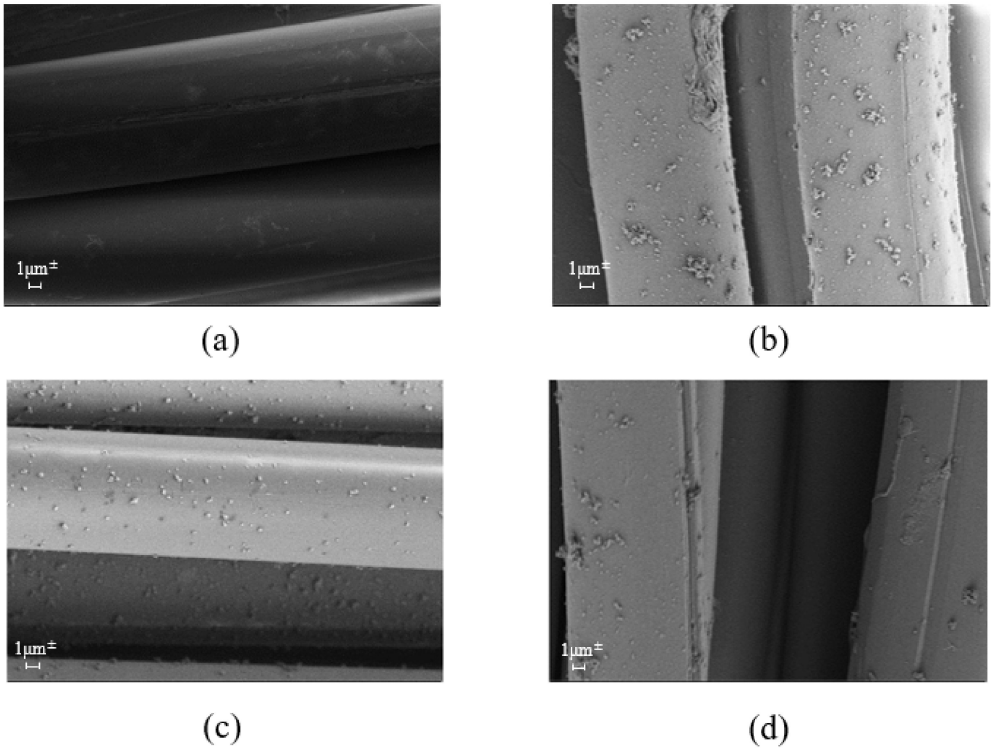

Figure 11. $ZnCl_2$-treated 6 h SEM image on the surface of the fiber. (**a**) 6 wt% $ZnCl_2$, (**b**) 6 wt% $ZnCl_2$ PDA, (**c**) 6 wt% PDA $ZnCl_2$ and (**d**) 10 wt% $ZnCl_2$ PDA.

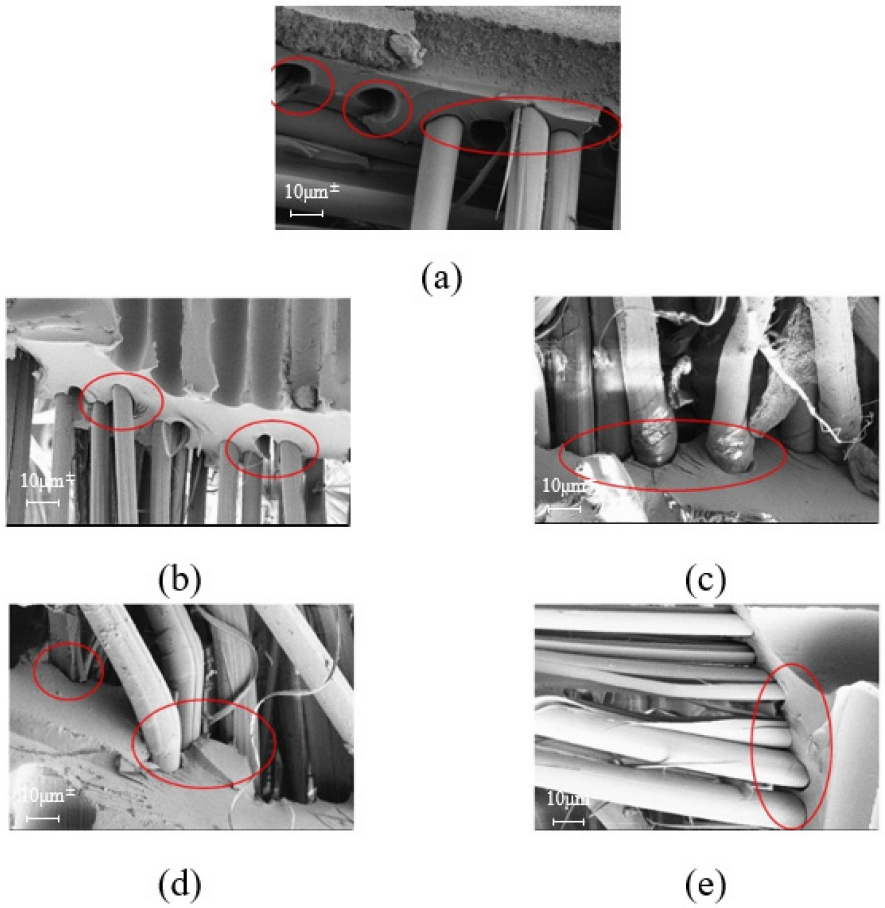

Figure 12. Fracture surface of each composites after the Impact test. (**a**) Untreated, (**b**) 6 wt% $ZnCl_2$, (**c**) 6 wt% $ZnCl_2$ PDA, (**d**) 6 wt% PDA $ZnCl_2$, (**e**) **10** wt% $ZnCl_2$ PDA.

4. Conclusions

In this study, the effect of the aramid fiber surface treatment on the mechanical performance and interfacial bonding of composites was investigated. The aramid fiber surface roughness was improved by performing a hybrid treatment of $ZnCl_2$ concentration, treatment time and PDA. All samples were manufactured by the VARTM process. As a result, the hybrid treatment of $ZnCl_2$ and PDA had an excellent effect on the mechanical properties of the composites.

I. The best tensile strength of 423.74 MPa was obtained at a $ZnCl_2$ concentration of 6 wt%, which is 3.51% higher than the untreated specimens. In addition, the tensile strength obtained at a $ZnCl_2$ concentration of 6 wt% was higher than that obtained at 10 wt%. Since the tensile strength is related to the properties of the fabric itself, the surface treatment did not have a significant effect on the tensile strength. It was also found that $ZnCl_2$ and PDA had negative and positive opposite effects on elongation, respectively. Additionally, these two treatments can effectively compensate for the mutual effects on AFRP, thus ensuring the mechanical properties of AFRP.

II. The bending strength under PDA-treated conditions reached the most excellent 247.85 MPa, which was 13% higher than that of the untreated specimens. Among the single treatments, the $ZnCl_2$ treatment showed the lowest improvement in performance while producing an etching effect on the surface fabric. All mixed treatments showed a decrease in performance in bending strength.

III. A concentration of 6 wt% $ZnCl_2$ and PDA treatment had the highest impact energy of 1.52 J was obtained for the hybrid treatment, which was more than 20% higher than the untreated condition. The impact power of the treated aramid

fiber composites was improved, where the mixed treatment condition increased by more than 8% compared to the single treatment condition. In the mixed treatment condition of $ZnCl_2$ and PDA, the higher impact work was obtained in the PDA treatment condition.

IV. The Lewis acid treatment increased the adhesion to the resin by etching the surface of the aramid fiber, but it had no effect on the tensile strength because it would damage the fabric itself. In the blend, the treatment had a positive effect on the impact work but had little effect on the tensile and flexural strengths.

V. According to the SEM observations, the higher the concentration of $ZnCl_2$ and the longer the treatment time, the better the etching effect on the fiber surface, but fiber separation occurs and reduces the mechanical properties. By observing the cross-sections of the composites, it was confirmed that the cross-sections under mixed treatment conditions were not treated or that the aromatic polyamide fibers were made denser with resin than the material with only a single treatment. The results show that the mixed treatment of $ZnCl_2$ and PDA can improve the mechanical properties of the composites.

Author Contributions: Conceptualization, G.X. and Y.J.; methodology, G.X.; software, G.X.; validation, G.X.; formal analysis, G.X.; investigation, G.X. and Y.J.; resources, J.S.; data curation, G.X.; writing—original draft preparation, G.X.; writing—review and editing, G.X., Y.J. and J.S. All authors have read and agreed to the published version of the manuscript.

Funding: This research was supported by the Basic Science Research Program through the National Research Foundation of Korea (NRF) funded by the Ministry of Education (NRF- 2018R1D1A1B07043528). The authors thank the Center for University-wide Research Facilities (CURF) at Jeonbuk National University for providing the characterization equipment and its instructions.

Institutional Review Board Statement: Not applicable.

Informed Consent Statement: Not applicable.

Data Availability Statement: Data generated by the FT-IR, FE-SEM and the mechanical properties are available in the form of text files by directly contacting the first author.

Conflicts of Interest: The authors declare no conflict of interest.

References

1. Shi, Z.; Zhang, S.; Wang, J.; Zhang, C.; Wang, Z.; Zou, B.; Zhang, X. Manufacturing method of aramid fiber applied to wearable intelligent system. *J. Alloys Compd.* **2021**, *869*, 159314. [CrossRef]
2. Zhang, B.; Jia, L.; Tian, M.; Ning, N.; Zhang, L.; Wang, W. Surface and interface modification of aramid fiber and its reinforcement for polymer composites: A review. *Eur. Polym. J.* **2021**, *869*, 110352. [CrossRef]
3. Yang, G.; Park, M.; Park, S. Recent progresses of fabrication and characterization of fibers-reinforced composites: A review. *Compos. Commun.* **2019**, *147*, 34–42. [CrossRef]
4. Hu, Y.; Liu, W.; Shi, Y. Low-velocity impact damage research on CFRPs with Kevlar-fiber toughening. *Compos. Struct.* **2019**, *216*, 127–141. [CrossRef]
5. Zhou, H.; Du, X.; Liu, H.; Zhou, H.; Zhang, Y.; Mai, Y. Delamination toughening of carbon fiber/epoxy laminates by hierarchical carbon nanotube-short carbon fiber interleaves. *Compos. Sci. Technol.* **2017**, *140*, 46–53. [CrossRef]
6. Lin, J.; Sun, C.; Min, J.; Wan, H.; Wang, S. Effect of atmospheric pressure plasma treatment on surface physicochemical properties of carbon fiber reinforced polymer and its interfacial bonding strength with adhesive. *Compos. Part B Eng.* **2020**, *199*, 108237. [CrossRef]
7. Kim, J.; Mauchauffe, R.; Kim, D.; Kim, J.; Moon, S. Mechanism study of atmospheric-pressure plasma treatment of carbon fiber reinforced polymers for adhesion improvement. *Surf. Coat. Technol.* **2020**, *393*, 125841. [CrossRef]
8. Cho, B.; Hwang, S.; Park, M.; Park, J.; Park, Y.; Chae, H. The effects of plasma surface treatment on the mechanical properties of polycarbonate/carbon nanotube/carbon fiber composites. *Compos. Part B Eng.* **2019**, *160*, 436–445. [CrossRef]
9. Lee, H.; Ohsawa, I.; Takahashi, J. Effect of plasma surface treatment of recycled carbon fiber on carbon fiber-reinforced plastics (CFRP) interfacial properties. *Appl. Surf. Sci.* **2015**, *328*, 241–246. [CrossRef]
10. Li, D.; Xiong, M.; Wang, S.; Chen, X.; Wang, S.; Zeng, Q. Effects of low-temperature plasma treatment on wettability of glass surface: Molecular dynamic simulation and experimental study. *Appl. Surf. Sci.* **2020**, *503*, 144257. [CrossRef]

11. Macedo, M.J.P.; Silva, G.S.; Feitor, M.C.; Costa, T.H.C.; Ito, E.N.; Melo, J.D.D. Surface modification of kapok fibers by cold plasma surface treatment. *J. Mater. Res. Technol.* **2020**, *9*, 2467–2476. [CrossRef]
12. Sarasini, F.; Tirillò, J.; Valente, M.; Ferrante, L.; Cioffi, S.; Iannace, S.; Sorrentino, L. Hybrid composites based on aramid and basalt woven fabrics: Impact damage modes and residual flexural properties. *Mater. Des.* **2013**, *49*, 290–302. [CrossRef]
13. Behera, A.; Behera, R.K.; Sahu, P.; Swain, R.R.; Mahapatra, T.R. Tensile and Failure Behavior of Kevlar Fiber Reinforced Epoxy Matrix Composite Exposed to Different Environmental Conditions. *Mater. Today Proc.* **2018**, *5*, 20250–20256. [CrossRef]
14. Zhong, J.; Luo, Z.; Hao, Z.; Guo, Y.; Zhou, Z.; Li, P.; Xue, B. Enhancing fatigue properties of styrene butadiene rubber composites by improving interface adhesion between coated aramid fibers and matrix. *Compos. Part B Eng.* **2019**, *172*, 485–495. [CrossRef]
15. Liu, L.; Huang, Y.; Zhang, Z.; Jiang, Z.; Wu, L. Ultrasonic treatment of aramid fiber surface and its effect on the interface of aramid/epoxy composites. *Appl. Surf. Sci.* **2008**, *254*, 2594–2599. [CrossRef]
16. Li, C.; Zhen, Q.; Luo, Z.; Lu, S. Effect of calcium chloride on the surface properties of Kevlar fiber. *Appl. Polym. Sci.* **2014**, *132*, 41358. [CrossRef]
17. Lv, J.; Cheng, Z.; Wu, H.; He, T.; Qin, J.; Liu, X. In-situ polymerization and covalent modification on aramid fiber surface via direct fluorination for interfacial enhancement. *Compos. Part B Eng.* **2020**, *182*, 107608. [CrossRef]
18. Lin, G.; Wang, H.; Yu, B.; Qu, G.; Chen, S.; Kuang, T.; Yu, K.; Liang, Z. Combined treatments of fiber surface etching/silane-coupling for enhanced mechanical strength of aramid fiber-reinforced rubber blends. *Mater. Chem. Phys.* **2020**, *255*, 123486. [CrossRef]
19. Xi, M.; Li, Y.; Shang, S.; Li, D.; Yin, Y.; Dai, X. Surface modification of aramid fiber by air DBD plasma at atmospheric pressure with continuous on-line processing. *Surf. Coat. Technol.* **2008**, *202*, 6029–6033. [CrossRef]
20. Jia, C.; Chen, P.; Liu, W.; Li, B.; Wang, Q. Surface treatment of aramid fiber by air dielectric barrier discharge plasma at atmospheric pressure. *Appl. Surf. Sci.* **2011**, *257*, 4165–4170. [CrossRef]
21. Kim, H.; Song, J. Improvement in the mechanical properties of carbon and aramid composites by fiber surface modification using polydopamine. *Compos. Part B Eng.* **2019**, *160*, 31–36. [CrossRef]
22. Xu, G. Improvement of Mechanical Properties by Surface Modification of $ZnCl_2$ and Polydopamine in Aramid Fiber Composites. Master's Thesis, Department of Energy Storage, Conversion Engineering of Graduate School, Jeonbuk National University, Jeonju, Korea, 2021.
23. *ASTM D638-14*; Standard Test Method for Tensile Properties of Plastic. ASTM: West Conshohocken, PA, USA, 2017.
24. *ASTM D790-17*; Standard Test Methods for Flexural Properties of Unreinforced and Reinforced Plastics and Electrical Insulating Materials. ASTM: West Conshohocken, PA, USA, 2017.
25. *ISO 179*; Plastics—Determination of Charpy Impact Properties. ISO: Geneva, Switzerland, 2020.
26. Norstrom, A.; Watson, H.; Engstrom, B.; Rosenholm, J. Treatment of E-glass fibres with acid, base and silanes. *Colloids Surf. A Phys. Chem. Eng. Asp.* **2001**, *194*, 143–157. [CrossRef]